

Identification of GSM and LTE Signals Using Their Second-order Cyclostationarity

Ebrahim Karami*, Octavia A. Dobre*, and Nikhil Adnani†

*Electrical and Computer Engineering, Memorial University, Canada
email: {ekarami,odobre}@mun.ca

† ThinkRF Corp., Ottawa, Canada
email: info@thinkrf.com

Abstract—Automatic signal identification (ASI) has various military and commercial applications, such as spectrum surveillance and cognitive radio. In this paper, a novel ASI algorithm is proposed for the identification of GSM and LTE signals, which is based on the pilot-induced second-order cyclostationarity. The proposed algorithm provides a very good performance at low signal-to-noise ratios and short observation times, with no need for channel estimation, and timing and frequency synchronization. Simulations and off-the-air signals acquired with the ThinkRF WSA4000 receiver are used to confirm the findings.

Index Terms—Global system of mobile (GSM), long term evolution (LTE), cyclostationarity.

I. INTRODUCTION

Automatic signal identification (ASI) has been initially investigated for military communications, e.g., for electronic warfare and spectrum surveillance [1]. More recently, ASI has found applications to commercial communications, in the context of software defined and cognitive radios [2], [3].

ASI tackles the problem of identifying the signal type without relying on pre-processing, such as channel estimation, and timing and frequency synchronization [1], [3]–[14]. While most of the ASI work in the literature has been done for generic signals, very few papers investigate the identification of standard signals; however, the latter is crucial for spectrum surveillance and cognitive radio applications. ASI techniques usually exploit signal features to identify the signal type [1], [4]–[13], and the feature-based identification of standard signals has been carried out as follows. In [4], the authors use second-order cyclostationarity-based features to classify different IEEE 802.11 standard signals. The pilot-induced cyclostationarity of the IEEE 802.11a standard signals is studied in [5], with ASI application. Kurtosis-based features are proposed in [6], [7] to identify OFDM-based standard signals. Furthermore, the cyclic prefix (CP)-, preamble-, and reference-signal-induced second-order cyclostationarity of LTE and WiMAX standard signals is exploited in [8]–[11] for

their identification. While the previously mentioned feature-based ASI techniques are developed for orthogonal frequency division multiplexing (OFDM)-based signals, they are not necessarily appropriate to other standard signals, such as GSM. Therefore, to identify such standard cellular signals, we need to develop ASI algorithms based on new features. In wireless communications systems, pilot signals are used for channel estimation, as well as frequency and timing synchronization. As the pilot symbols are sent periodically, one can use this periodicity to identify different wireless standard signals. In this paper, we propose a low complexity algorithm to identify the GSM and LTE standard signals, as being widely used in Canada; off-the-air signals are used for verification.

The rest of the paper is organized as follows. Section II presents the model for the GSM and LTE standard signals. Section III introduces the proposed algorithm for the identification of these signals. In Section IV, results for off-the-air signals acquired with the ThinkRF WSA4000 receiver are shown, along with simulation results. The paper is concluded in Section V.

II. SIGNAL MODEL

In this section, the signal model for the GSM and LTE downlink (DL) is introduced. More specifically, we present the pilot signals in these standards, as their periodicity will be exploited for the identification feature.

A. GSM Signal Model

The GSM frame structure is shown in Fig. 1, including the normal burst, which carries data, the control bursts, such as frequency correction and synchronization, as well as the access bursts [15]. In the normal burst, 26 bits in each time slot are dedicated to training; these are repeated every time slot and used for channel estimation. Since the duration of each time slot is $577 \mu\text{s}$, the repetition frequency of the pilot sequence is 1733 Hz. From Fig. 1, one can see that the other GSM bursts have similar repetitive sequences, but with different lengths; however, all repeat with the same frequency, i.e., 1733 Hz.

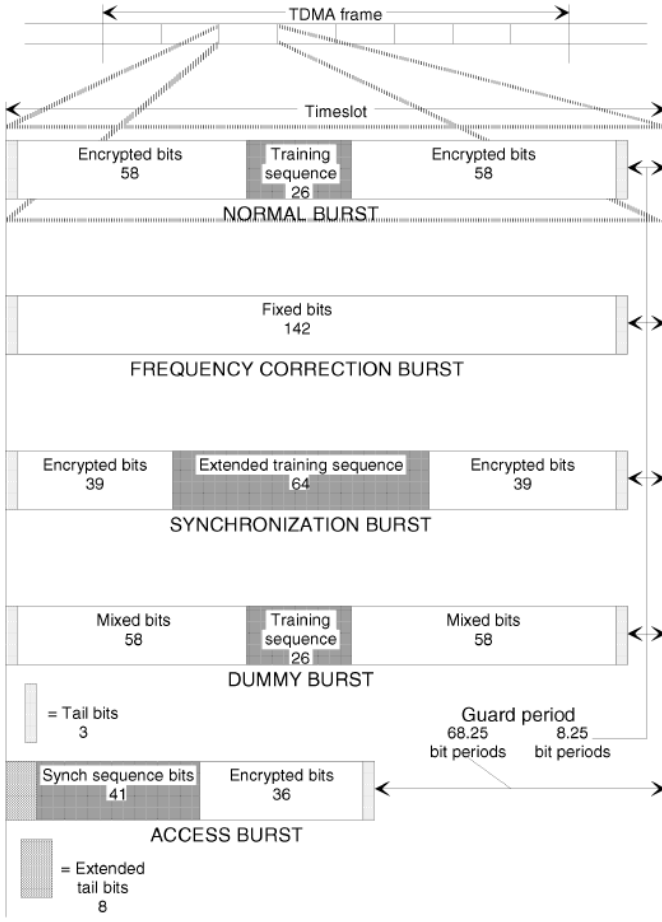


Fig. 1. Time slot and format of bursts in the GSM systems [15].

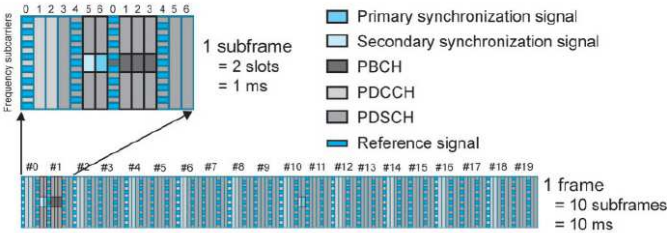


Fig. 2. LTE FDD DL frame structure [17].

B. LTE DL Signal Model

The LTE frequency division duplex (FDD) DL frame structure is shown in Fig. 2. Each LTE frame includes 20 time slots, each with 6 or 7 OFDM symbols, depending if the short or long CP is used [16]. In Canada, LTE with short CP is commonly employed. From Fig. 2, one can see that the samples which are periodically repeated correspond to the cell specific reference signals (RSs), and primary and secondary synchronization channels (PSCH and SSCH), where the RS is repeated every time slot and PSCH and SSCH are repeated every 10 time slots. The duration of each LTE time slot is 0.5 ms. Consequently, the repetition frequency for the RSs is 2 kHz, while for the PSCH and SSCH is 200 Hz.

III. PROPOSED SIGNAL IDENTIFICATION ALGORITHM

In this section, the algorithm proposed for the identification of GSM and LTE standard signals is presented. First, we introduce the fundamental concept of signal cyclostationarity in order to further discuss the identification feature, and then present the feature-based algorithm and study its complexity.

A. Second-order Signal Cyclostationarity

A signal $r(t)$ exhibits second-order cyclostationarity if its first and second-order time-varying correlation functions are periodic in time [18]. In this work, the following second-order time-varying correlation function is considered

$$c(t, \tau) = E[r(t)r^*(t + \tau)], \quad (1)$$

where $*$ denotes complex conjugation, $E[\cdot]$ is the statistical expectation, and τ is the delay. If $c(t, \tau)$ is periodic in time with the fundamental period M_0 , then it can be expressed by a Fourier series as [18]

$$c(t, \tau) = \sum_{\{\alpha\}} C(\alpha, \tau) e^{j2\pi t\alpha}. \quad (2)$$

The Fourier coefficients defined as

$$C(\alpha, \tau) = \frac{1}{M_0} \int_0^{M_0} c(t, \tau) e^{-j2\pi t\alpha} dt, \quad (3)$$

are referred to as the cyclic correlation function (CCF) at cyclic frequency (CF) α and delay τ . The set of CFs is given by $\{\alpha\} = \{\frac{\ell}{M_0}, \ell \in \mathcal{I}, \text{ with } \mathcal{I} \text{ as the set of integers}\}$. Assuming M_r as the number of received samples, CCF at CF α and delay τ is estimated from the received sequence, $r(m)$, as [19]

$$\hat{C}(\alpha, \tau) = \frac{1}{M_r} \sum_{m=0}^{M_r-1} r(m)r^*(m + \frac{\tau}{T_s}) e^{-j2\pi \alpha m T_s}. \quad (4)$$

where T_s is the sampling period and τ is multiple integer of T_s .

Due to the periodicity of the pilot signals in GSM and LTE standards, one can show that these induce second-order cyclostationarity with CFs $\alpha_i = \frac{\ell}{T_i}$, $i = \text{GSM, LTE}$, where T_i is the time slot duration of the GSM and LTE standards. The pilot-induced second-order cyclostationarity will be used as an identification feature, as presented in the next sub-section.

B. Proposed Second-order Cyclostationarity-based Algorithm

We explore the CCF at CF α and zero delay $C(\alpha, 0)$ to identify the GSM and LTE standard signals, as follows. In the first step, $\hat{C}(\alpha, 0)$ is estimated at CFs $\alpha_i = \frac{1}{T_i}$, $i = \text{GSM, LTE}$. In the second step, the estimated CCF magnitude is compared with a threshold, which is set up based on a constant false

alarm criterion. The probability of false alarm is defined as the probability of deciding that the standard signal is present when this is not (either an unknown signal or noise is present). An analytical closed form expression of the false alarm probability is obtained based on the distribution of the CCF magnitude estimate for the unknown signal and noise; in this case, one can simply infer that the CCF magnitude estimate has an asymptotic Rayleigh distribution [19]. Hence, if the CCF for a specific CF α and delay τ is used as a discriminating feature, the probability of false alarm is calculated using the complementary cumulative density function of the Rayleigh distribution as

$$P_F = \exp\left(-\frac{\Gamma^2}{\sigma_r^2}\right), \quad (5)$$

where σ_r^2 is the variance of the received signal. A summary of the proposed algorithm is provided as follows.

Proposed algorithm

Input: The received sequence $r(m)$, $m = 0, \dots, M_r - 1$.
- Estimate the CCF, $C_i = \hat{C}(\alpha_i, 0)$, using (4) at CFs $\alpha_i = \frac{1}{T_i}$, $i = \text{GSM, LTE}$.
- Estimate the variance of the received signal, σ_r^2 , and calculate the threshold using (5).
if $C_i > \Gamma$ **then**
- The received signal is identified as i , $i = \text{GSM, LTE}$.
else
- The type of the received signal is not i and it can be either an intruder or noise.
end if

Computational complexity: We evaluate the computational complexity of the proposed identification algorithm through the number of floating point operations (flops) [20], where a complex multiplication and addition require six and two flops, respectively. Based on (4), one can easily see that the number of complex multiplications and additions needed to calculate the CCF equals $2M_r$ and $M_r - 1$, respectively. By considering that the thresholding does not require additional complexity, it is straightforward that the number of flops needed by the algorithm equals $14M_r - 2$. It is worth noting that with an average Intel Core i750, the identification process takes 68.5 ms for $M_r = 50000$; hence, the algorithm can be implemented in practice.

IV. RESULTS

In this section, the results for simulated and off-the-air signals are presented.

A. CCF for Simulated Signals

Here we present simulation results for the CCF magnitude of the GSM and LTE signals. For each case, a signal burst of 1000 time slots is generated and then transmitted through a frequency-selective fading channel consisting of $L_p = 4$

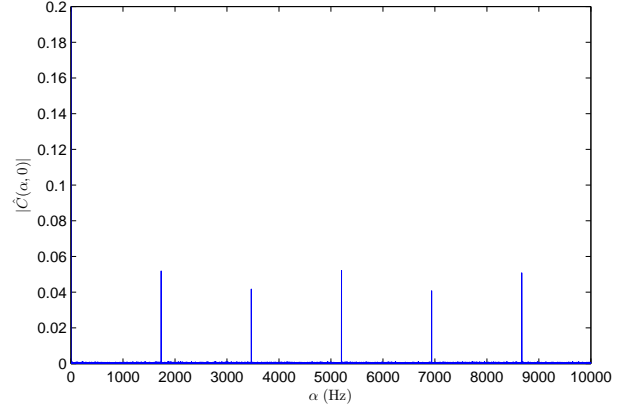


Fig. 3. CCF magnitude vs. CF for simulated GSM signals.

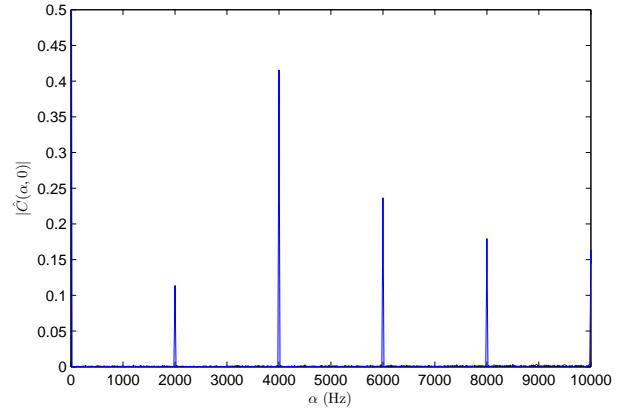


Fig. 4. CCF magnitude vs. CF for simulated LTE signals.

statistically independent taps, each being a zero-mean complex Gaussian random variable. The channel is characterized by an exponential power delay profile, $\sigma^2(p) = B_h \exp(-p/5)$, where $p = 0, \dots, L_p - 1$ and B_h is chosen such that the average power is normalized to unity and SNR is 20 dB. Fig. 3 presents simulation results for the GSM signals, while Fig. 4 shows results for the LTE signals. As expected, one can easily see that the CCF obtained from the simulated GSM signal has peaks at CFs equal to multiple integers of 1733 Hz, which is the reciprocal of the GSM time slot duration. Furthermore, also as expected, the estimated CCF for the simulated LTE signal has peaks at CFs equal to multiple integers of 2 kHz, which is the reciprocal of the LTE time slot duration.

B. CCF for Off-the-air Signals

In this section, results for the CCF magnitude estimated from the signals received by a WSA4000 receiver is presented. The location of measurements was the ThinkRF company, in the north Kanata area of Ottawa, Canada. For each frequency band, 10^6 samples were received. The bandwidth of the signal received by the WSA4000 receiver was 125 MHz, and the system had a decimation rate parameter to decrease the bandwidth; as such, depending on the expected bandwidth

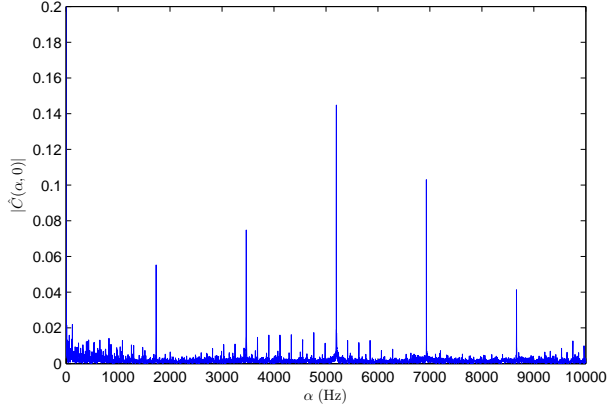


Fig. 5. CCF magnitude vs. CF for a signal received by the WSA4000 system within the frequency band of 869 MHz.

of the received signal, an appropriate decimation factor was considered. Please note that the proposed algorithm does not need to know the exact bandwidth of the received signal; as long as the signal of interest is in the bandwidth of the received signal, the proposed algorithm can identify it.

Fig. 5 presents the CCF magnitude results for the signal in the 869 MHz band, where we expect the GSM signal from the Rogers base station (BS) located at approximately 460 meter away from our receiver. The decimation factor for this measurement was 64, corresponding to a 1.951 MHz receive bandwidth. This bandwidth was enough to cover the GSM bands supported by the corresponding BS¹. From Fig. 5, one can see that the CCF estimated from the off-the-air GSM signal has peaks at CFs equal to multiple integers of 1733 Hz, which agrees with the simulation results.

Fig. 6 presents the CCF magnitude results for the signal in the 2115 MHz band, where we expect the LTE signal from the Rogers BS located at approximately 460 meter away from the receiver (the location of this BS is the same as in the previous case). The decimation factor for this measurement was 16, corresponding to a 7.81 MHz receive bandwidth, which covers the LTE signal transmitted by the BS. From Fig. 6, one can see that the CCF estimated from the off-the-air LTE signal has peaks at CFs equal to multiple integers of 2 kHz, which concurs with the simulation results.

C. Performance of the Proposed Algorithm

In this section, the performance of the proposed algorithm for the identification of GSM and LTE signals is evaluated by Monte Carlo simulation through averaging over 1000 iterations. The simulation parameters are the same as in subsection IV-A. The threshold is set up based on the constant false alarm criterion, and in each iteration, data is generated with a random timing offset taken from a uniform distribution within the first time slot.

¹Each GSM band is 200 kHz.

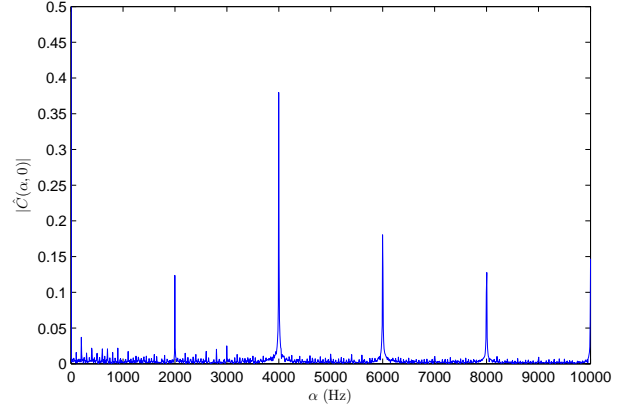


Fig. 6. CCF magnitude vs. CF for a signal received by the WSA4000 system within the frequency band of 2115 MHz.

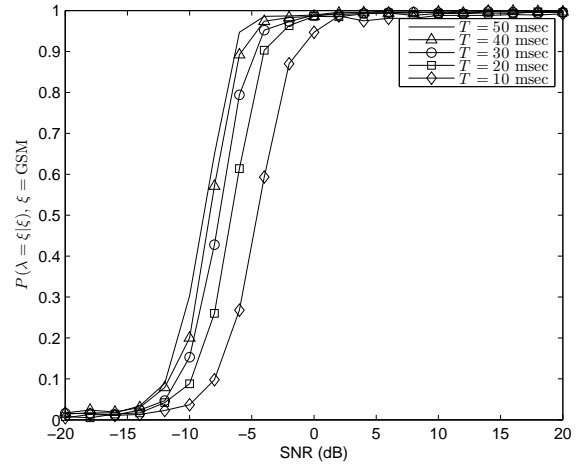


Fig. 7. Probability of correct identification for the GSM signals, $P(\lambda = \xi|\xi)$, $\xi = \text{GSM}$, versus SNR for different observation times, T .

Fig. 7 presents the performance of the proposed algorithm for the identification of the GSM signals for different observation times, with $P_F = 10^{-2}$. From Fig. 7, one can see that with $\text{SNR} > 0$ dB, the probability of correct identification, $P(\lambda = \text{GSM}|\text{GSM})$, approaches one at an observation time as low as 10 ms, while with 50 ms, this occurs at about -5 dB SNR. Fig. 8 presents the performance of the proposed algorithm for the detection of the LTE signals for different observation times, with $P_F = 10^{-2}$. From Fig. 8, one can notice that with $\text{SNR} > -5$ dB, the probability of correct correct identification, $P(\lambda = \text{LTE}|\text{LTE})$, approaches one at an observation time as low as 10 ms. In all cases, the results obtained for the LTE signal is better than for the GSM signal; however, one can obtain a good performance at short observation times and with low SNR for both signal types.

Fig. 9 presents the performance of the proposed algorithm for the identification of the GSM and LTE signals for different P_F values, with an observation time of $T = 10$ ms. From Fig. 9, one can see that for LTE signals with $\text{SNR} > -5$ dB, a very

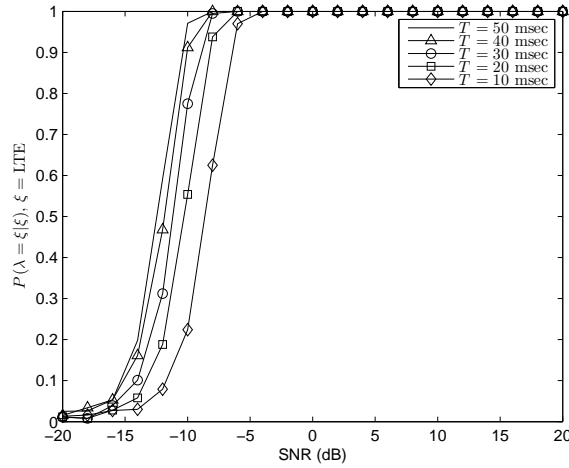


Fig. 8. Probability of correct identification for the LTE signals, $P(\lambda = \xi|\xi)$, $\xi = \text{LTE}$, versus SNR for different observation times, T .

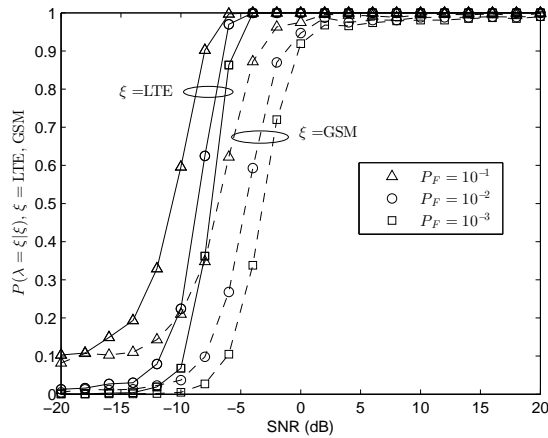


Fig. 9. Probability of correct identification for the GSM and LTE signals, $P(\lambda = \xi|\xi)$, $\xi = \text{GSM, LTE}$, versus SNR for different P_F values. Solid lines are used for the LTE signal and dashed lines are used for the GSM signal.

good performance is achieved regardless of the P_F value; at lower SNRs, it is observed that $P(\lambda = \text{LTE}|\text{LTE})$ improves as P_F increases. For the GSM signal, $P(\lambda = \text{GSM}|\text{GSM})$ approaches one for $\text{SNR} > 0$ dB regardless of the P_F value; at lower SNRs, the performance also enhances as P_F increases. In all cases, a better performance is attained for LTE signal identification when compared with GSM.

V. CONCLUSION

In this paper, we proposed a very low complexity second-order cyclostationarity based algorithm for the identification of the GSM and LTE standard signals, which are commonly used in Canada. The proposed algorithm attains a very good performance at low SNRs and with short observation times. Signals acquired by a ThinkRF WSA4000 receiver were used to prove the concept.

ACKNOWLEDGMENT

The authors would like to acknowledge Tim Hember and Dr. Tarek Helaly from ThinkRF Corp. for their kind support.

REFERENCES

- [1] O. A. Dobre, A. Abdi, Y. Bar-Ness, and W. Su, "A Survey of Automatic Modulation Classification Techniques: Classical Approaches and New Developments," *IET Communications*, vol. 1, pp. 137–156, Apr. 2007.
- [2] J. Mitola and G. Maguire, "Cognitive Radio: Making Software Radios More Personal," *IEEE Personal Communications*, vol. 6, no. 4, pp. 13–18, Aug. 1999.
- [3] T. Yucek and H. Arslan, "A Survey of Spectrum Sensing Algorithms for Cognitive Radio Applications," *IEEE Communications Surveys and Tutorials*, vol. 11, no. 1, pp. 116–130, Mar. 2009.
- [4] K. Kim, C. M. Spooner, I. Akbar, and J. H. Reed, "Specific Emitter Identification for Cognitive Radio with Application to IEEE 802.11," in *Proc. IEEE Global Telecommunications Conference*, 2008, pp. 1–5.
- [5] M. Adrat, J. Leduc, S. Couturier, M. Antweiler, and H. Elders-Boll, "2nd Order Cyclostationarity of OFDM Signals: Impact of Pilot Tones and Cyclic Prefix," in *Proc. IEEE International Conference on Communications*, 2009, pp. 1–5.
- [6] A. Bouzegzi, P. Jallon, and P. Ciblat, "A Fourth-order Based Algorithm for Characterization of OFDM Signals," in *Proc. IEEE SPAWC*, 2012, pp. 411–415.
- [7] A. Bouzegzi, P. Ciblat, and P. Jallon, "New Algorithms for Blind Recognition of OFDM Based Systems," *ELSEVIER: Signal Processing*, vol. 90, pp. 900–913, Mar. 2010.
- [8] A. Al-Habashna, O. A. Dobre, R. Venkatesan, and D. C. Popescu, "WiMAX Signal Detection Algorithm Based on Preamble-induced Second-order Cyclostationarity," in *Proc. IEEE Global Telecommunications Conference*, 2010, pp. 1–5.
- [9] —, "Cyclostationarity-based Detection of LTE OFDM Signals for Cognitive Radio Systems," in *Proc. IEEE Global Telecommunications Conference*, 2010, pp. 1–6.
- [10] —, "Second-Order Cyclostationarity of Mobile WiMAX and LTE OFDM Signals and Application to Spectrum Awareness in Cognitive Radio Systems," *IEEE Journal of Selected Topics in Signal Processing*, vol. 6, no. 1, pp. 26–42, Feb. 2012.
- [11] —, "Joint Cyclostationarity-based Detection and Classification of Mobile WiMAX and LTE OFDM Signals," in *Proc. IEEE International Conference on Communications*, 2011, pp. 1–6.
- [12] W. Gardner and C. Spooner, "Signal Interception: Performance Advantages of Cyclic-Feature Detectors," *IEEE Transactions on Communications*, vol. 40, no. 1, pp. 149–159, Jan. 1992.
- [13] A. Punchihewa, Q. Zhang, O. A. Dobre, C. Spooner, and R. Inkol, "On the Cyclostationarity of OFDM and Single Carrier Linearly Digitally Modulated Signals in Time Dispersive Channels: Theoretical Developments and Application," *IEEE Transactions on Wireless Communications*, vol. 9, pp. 2588–2599, Mar. 2010.
- [14] W. Su, J. Xu, and M. Zhou, "Real-time Modulation Classification Based On Maximum Likelihood," *IEEE Communications Letters*, vol. 12, no. 11, pp. 801 – 803, Nov. 2008.
- [15] European Telecommunications Standard Institute (ETSI), Rec. ETSI/GSM 05.02, *Multiplexing and Multiple Access on the Radio Path*, version 3.5.1, Mar. 1992.
- [16] A. Ghosh, J. Zhang, J. Andrews, and R. Muhamed, *Fundamentals of LTE*. Prentice Hall, 2010.
- [17] M. Rumney, *LTE and the Evolution to 4G Wireless: Design and Measurement Challenges*, 2nd Edition, 2nd ed. Wiley, 2013.
- [18] W. Gardner and C. Spooner, "The Cumulant Theory of Cyclostationary Time-Series, Part I. Foundation," *IEEE Transactions on Signal Processing*, vol. 42, no. 12, pp. 3387–3408, Dec. 1994.
- [19] A. Dandawate and G. Giannakis, "Statistical Tests for Presence of Cyclostationarity," *IEEE Transactions on Signal Processing*, vol. 42, no. 9, pp. 2355–2369, Sep. 1994.
- [20] S. Watkins, *Fundamentals of Matrix Computations*. Wiley, 2002.